



Isotopic and hydrogeochemical evaluation of springs discharging from high-elevation karst aquifers in Lar National Park, northern Iran

Abdollah Shamsi¹ · Gholam Hossein Karami¹ · Daniel Hunkeler² · Azizollah Taheri¹

Received: 17 March 2018 / Accepted: 31 August 2018 / Published online: 27 October 2018
© Springer-Verlag GmbH Germany, part of Springer Nature 2018

Abstract

Stable isotopes oxygen-18 ($\delta^{18}\text{O}$) and deuterium (δD) and the hydrochemistry of the main springs of well-developed karst aquifers in Lar watershed in the Haraz basin, northern Iran, were investigated. Water samples were collected in the recession period for analysis of major ions and the stable isotopes. Predominant hydrochemical types of main karst springs samples were $\text{Ca}^{2+} - \text{Mg}^{2+} - \text{HCO}_3^-$ type. The hydrochemical composition of the karst springs is dominated by Ca^{2+} , Mg^{2+} , HCO_3^- and SO_4^{2-} ions. The hydrochemical results indicate that dissolution of carbonate rocks (limestone and dolomite) governs the major ion concentrations, with minor effects of silicate weathering, ion exchange and precipitation effects on concentrations of Na^+ , Cl^- , K^+ , and SO_4^{2-} . In the northern parts of the study area, hydrothermal fluid affects the chemistry of the draining springs. The isotopic content ranges from -43.8 to -52.9‰ and from -7.09 to -8.97‰ for δD and $\delta^{18}\text{O}$, respectively. The karst spring samples lie above the local meteoric water line, similar to the $\delta^{18}\text{O}$ and δD signature of the snowpack samples, and have small spatial and temporal variability. The similarity of the isotopic composition of the springs to the snowpack suggests that the dominant recharge is by snowmelt water.

Keywords Stable isotope · Karst spring · Hydrochemistry · Iran

Introduction

Groundwater is the most significant contributor to the water supply in semiarid parts of the world and has incredible societal and economic influences especially during the summer and during prolonged drought. Sustainable and effective groundwater resources management and implementation of their appropriate protection require a comprehensive understanding of the aquifer characteristics (Raghavendra and Deka 2015). Karst aquifers are one of the main groundwater resources; 25% of the world population depends upon this kind of aquifer (Ford and Williams 2007). Further, these landscapes almost always contain considerable quantities of high quality water.

In high mountainous aquifers, there are often no exploration wells or they are sparsely distributed. Springs can provide valuable information about both local and regional hydrogeology (Larsen et al. 2001; Andreo et al. 2002). Karst spring discharge is the result of the interaction between climatological factors (recharge characteristics), the geometry of the catchment area, and the degree of karstification involving carbonate formations (Padilla et al. 1994; Raeisi and Karami 1996; Fiorillo 2014; Miao et al. 2014; Malík 2015).

High temporal and spatial heterogeneity is a common characteristic of karst landscapes (Padilla et al. 1994; Turk et al. 2015; Fu et al. 2015; Jukić and Denić-Jukić 2015; Poulain et al. 2015). Therefore, it is a challenging task to acquire precise data about these aquifers (Birk et al. 2004). Full understanding of a karstic aquifer system is a time-consuming, expensive and difficult process (Stevanovic 2015) and nearly impossible in some cases due to the difficulty of direct measurement of the characteristics (Padilla et al. 1994; Tang et al. 2015). Accordingly, use of different tools and methods that can provide any information about these systems will be valuable.

In the past few decades, researchers frequently applied hydro-geochemistry and stable isotopes in some cases coupled with other hydrogeological method for many different purposes

✉ Abdollah Shamsi
a.shamsi@shahroodut.ac.ir

¹ Faculty of Earth Sciences, Shahrood University of Technology, Shahrood, Iran

² Center for Hydrogeology and Geothermics (CHYN), University of Neuchâtel, Neuchâtel, Switzerland

(e.g., Doctor and Alexander 2005; Bhat and Jeelani 2015; Hamdan et al. 2016; Dursun et al. 2016). Hydrochemistry and stable isotopes provide valuable information about the sources, timing and groundwater recharge areas, water–rock interactions through the flow paths, and mixing of different groundwater bodies (Larsen et al. 2001; Kohfahl et al. 2008; Kanduč et al. 2012; Pu et al. 2013). Hydrochemistry and stable isotopes are employed for hydrograph separation (Doctor et al. 2006; Klaus and McDonnell 2013; Hatipoglu-Bagci and Sazan 2014). Likewise, delineation of the recharge area and distinguishing sources of recharge to the karst springs have been accomplished by applying stable isotopes and hydrochemistry (Blasch and Bryson 2007; Seeyan and Merkel 2014; Bhat and Jeelani 2015).

The primary objective of this research is to characterize the general hydrogeology of the main karst springs in the Lar watershed in the north of Iran. In this regards, hydrochemistry of major ions and stable isotopes ($\delta^{18}\text{O}$ and δD) of the main karst springs in Lar watershed were investigated. Besides this, spatial and temporal variability of the isotope signature and hydrochemistry were evaluated at the basin scale.

Study area

The study area is located in the western part of the Polour district of the Mazandran province in Iran, and it extends between $35^{\circ}50'$ and $36^{\circ}05'N$, and $51^{\circ}34'$ and $52^{\circ}06'E$, 70 km northeast of Tehran (Fig. 1). The Lar catchment area is situated in the southwestern parts of the Haraz basin, which is located in the Central Alborz mountain range. The total sub-basin extent

is 784 km^2 coinciding mostly with the Lar National Park. The entire catchment area has relatively steep topography with an average slope of 22° . Surface elevation varies between 2,300 and 5,670 m above sea level (a.s.l.), with an average elevation of 3,113 m a.s.l. Most of the higher elevation area is dominated by V-shaped valleys with steep slopes, whereas alluvial deposits that cover the flood plain of the main rivers have a gentle slope. The common land use of the watershed is grazing by sheep in summer and a few small farmlands in the flood plain of Lar River, which is cultivated on a seasonal basis.

Geological setting and tectonic outline

From the geological point of view, the study area is situated on the southern flank of the Central Alborz domain in the Alborz Mountain Range. Central Alborz is a part of the Alpine–Himalayan orogeny belt (Stocklin 1968; Alavi 1996) that evolved by different orogeny during the Cimmerian and Alpine orogeny (Alavi 1996; Zanchi et al. 2009). Such geological events resulted in an extremely complex geology and asymmetric structures (Stocklin 1968); however, the Cenozoic compressional events masked almost all of the earlier structural events data, and the majority of the geological structures (folds and fault) are oriented with a NWW–SEE and E–W trend (Zanchi et al. 2009).

The Lar watershed consists of the Lower Jurassic to Paleocene sedimentary and volcanic rocks (Fig. 2). The Shemshak formation (Lower Jurassic) consists of sandstone, shale, and siltstone, with limited outcrop at the central part of the watershed; it is the oldest formation and it acts as a basement

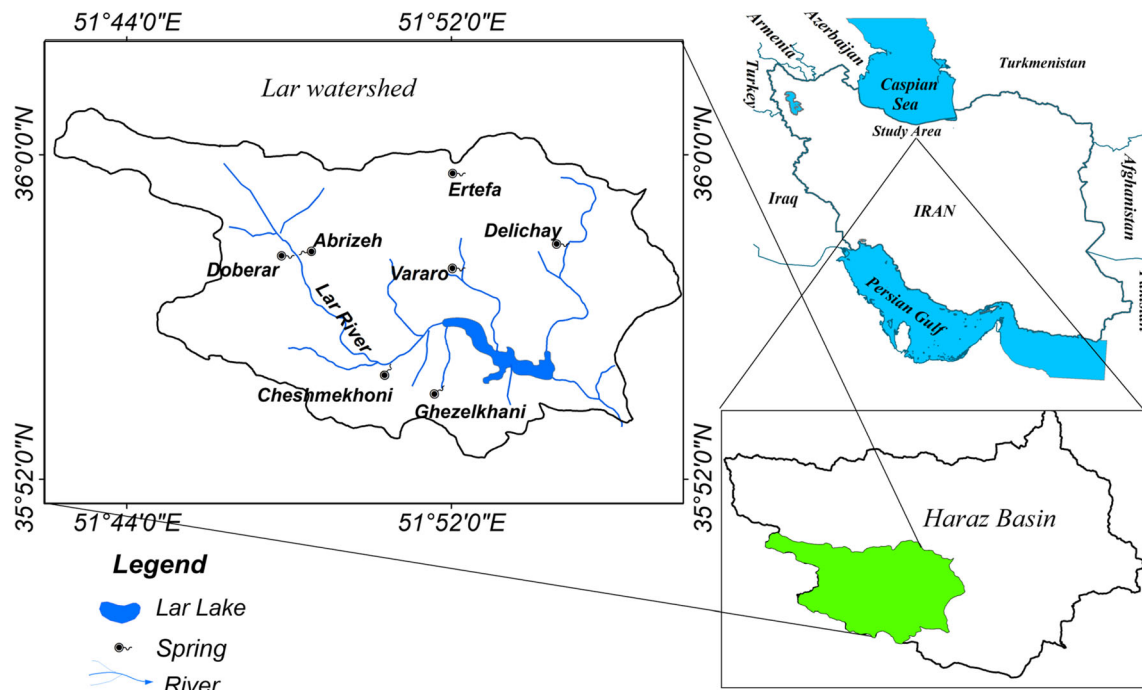


Fig. 1 Geographical location of the study area showing the main karst springs

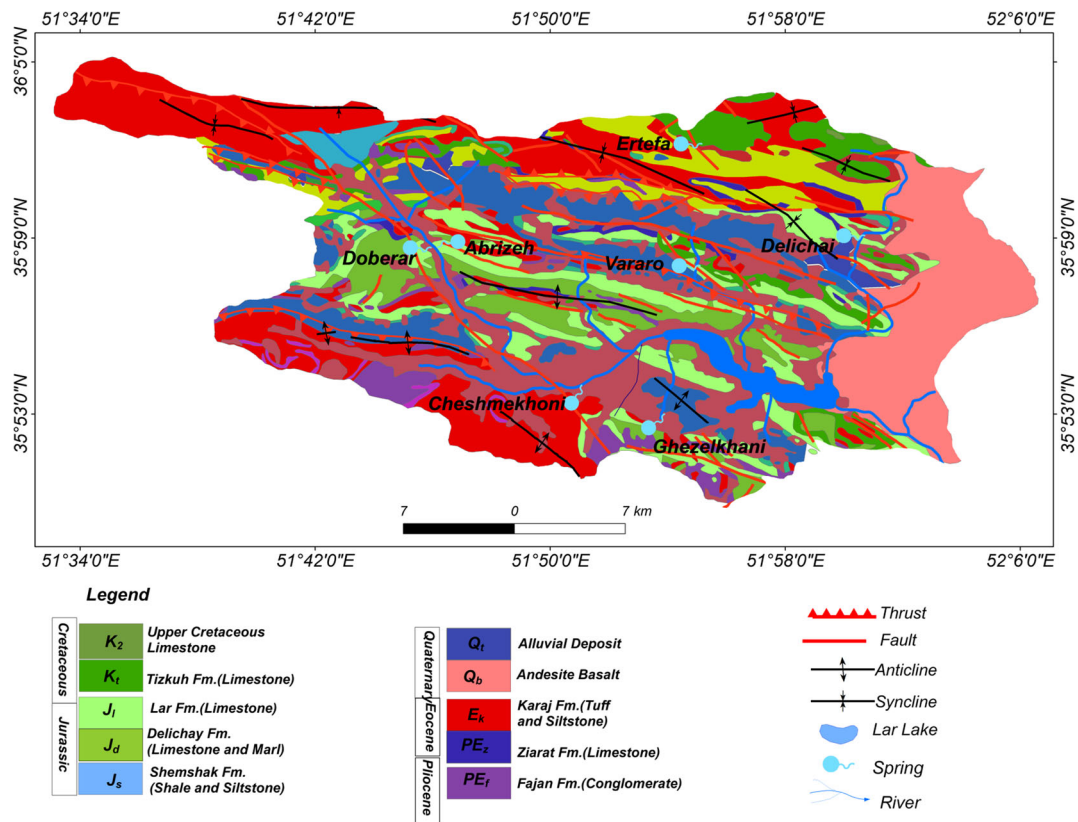


Fig. 2 Geological map of the Lar watershed

for the study area. Delichay formation (Middle Jurassic) predominantly consists of marly thin-bedded limestone. Lar formation (Upper Jurassic) is composed of medium-thick-bedded limestone, and the thickness of this formation in some part is up to 893 m (Alavi 1996). Tiz-Kuh formation (Early Cretaceous) has unconformity and overlies the Lar limestone, and it comprises a fine-grained massive limestone. The Cenozoic strata consists of the Fajan, Ziarat and Karaj formations in ascending stratigraphic order. During the Paleocene, the Fajan conglomerate was deposited over the older formations and is followed by deposition of Nummulitic limestone (Ziarat Formation) during Eocene, which has been covered by Karaj formation (late Eocene), mostly consisting of green tuffs, sandstones, shale and minor conglomerates. Damavand volcano includes mainly trachyandesites erupted in early Pleistocene and covers the older sedimentary rocks (Davidson et al. 2004; Shabanian et al. 2012). Quaternary alluvial deposits superimpose almost all of the Lar and Delichay valley floors near the Lar Dam site.

Hydrology and hydrogeology

The hydrologic cycle of the high-elevation Lar watershed is characterized by a dominant snow accumulation period during late autumn and winter, which is followed by a snowmelt runoff period during late spring, and a few rain events in the spring and

summer. The mean amount of precipitation, based on the 10-year statistics from 1967 to 1987 at 10 stations in the catchment, is about 700 mm annually. The precipitation increases with elevation, so that for every 1,500-m increase of elevation, the recorded amount of precipitation is doubled (Kazemi 2003). The precipitation falls unequally between October and May, with the highest amount in February, March and April, at about 300 mm for these 3 months. Lar and Delichay rivers are permanent and they are the most important drainage networks of the watershed. Stream flow in late summer and early autumn is predominately base flow; however, the potential for storm flow from heavy rainfall exists.

Hydrogeologically, the study area may be considered as a karstic landscape due to considerable outcrops of carbonate formations (Fig. 2), which discharge almost always in a natural way at 25 springs—discharge (Q) more than 20 L/s—in permanent and intermittent forms. Some small alluvial aquifers exist in the flood plain of the main rivers that are connected to the karst aquifers. The karst aquifers show very different characteristics compared to the other aquifer systems in the region because of their geological structure, the geometry of the catchment area, the thickness of the vadose zone, the hydraulic gradient and the degree of karstification. Generally, the springs can be classified based on the type of occurrence, as overflow type or contact drainage type. Discharge of these springs ranges between 20 and 2,500 L/s, and the spatial and temporal variability of discharge is up to 200%. Figure 3 shows the spatial locations of the

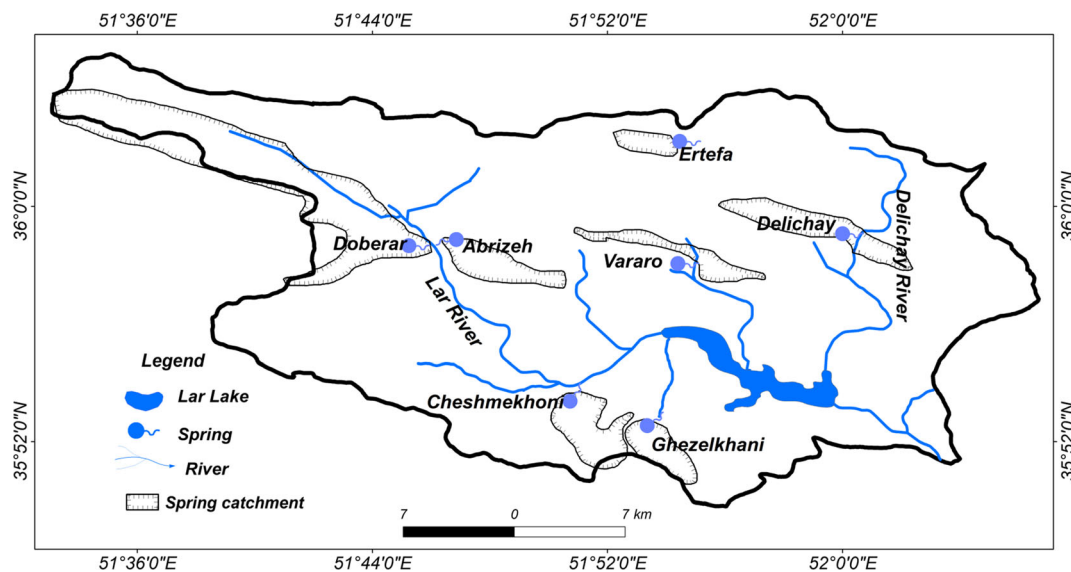


Fig. 3 Locations of the main karst spring and their possible catchment areas

main karst springs as well as their estimated catchment areas, based on annual discharge data and geological conditions.

Materials and methods

Out of the 25 springs in Lar catchment, 7 main karst springs with a higher amount of discharge were selected for in situ measurements and sampling for hydrochemical and stable isotope analysis. Since the area is not accessible from the late autumn to the late spring, sampling and measurements of the karst springs were performed during the recession period from June 2015 to October 2015. During the first 3 months, measurements and sampling were carried out at biweekly intervals and on a monthly basis in the last month. Springs discharge, water temperature (T) and electrical conductivity (EC) were measured in the field. Electrical conductivity and water temperature were measured at each spring's outlet with a WP-84 TPS conductivity meter and certified mercury-thermometer with an accuracy of $0.01 \mu\text{S}/\text{cm}$ and $0.1 \text{ }^\circ\text{C}$ respectively. The samples for stable isotope analysis were collected in 70-ml polyethylene dark bottles with airtight caps following the standard procedures (Clark and Fritz 1997). Bottles were rinsed in spring water several times and then filled to the top to minimize entrapment of air. The samples were not filtered and were collected at the spring outlet. Likewise, the sampling for the chemistry analysis was carried out by the standard methods in 500-ml bottles. Monthly precipitation samples were collected at the Lehra (3,300 m a.s.l.) and Druk (2,700 m a.s.l.) stations at accessible points in the north of the Lar watershed for evaluation of precipitation isotope contents.

The stable isotopic contents of spring water samples were measured by high-precision laser spectroscopy (Picarro L2130) at the laboratory of Center for Hydrogeology and Geothermic at Neuchatel University (CHYN), Switzerland. Analytical

precision is ± 0.08 and $\pm 0.9\text{‰}$ for $\delta^{18}\text{O}$ and for δD isotope ratios, respectively. The cations (NH_4^+ , Na^+ , K^+ , Mg^{2+} , Ca^{2+}) were analyzed with a Dionex DX-120 ion chromatograph and the anions (Cl^- , NO_3^- , SO_4^{2-}) were measured with a Dionex ICS-1600 ion chromatograph with a detection limit of $0.1 \text{ mg}/\text{L}$. Bicarbonate was measured with a 848 Titrimo plus, working with HCl 0.1 M for titration. Total dissolved solids (TDS) were calculated as the sum of the aforementioned ion species. It should be noted that strontium, fluoride, nitrite, bromide, phosphate, lithium, and ammonium were below the mechanism's detection limits (data not shown).

Results

Chemical composition of the main karst springs

The results of hydrochemical analysis of the seven main karst springs are summarized in Table 1. Figure 4a, b shows the Schoeller and Piper diagrams (Piper 1944) of the karst springs samples. Generally, the Ertefa spring has the lowest ion concentrations and the Vararo and Delichay springs have the highest ion concentrations (Fig. 4a). HCO_3^- , Ca^{2+} , SO_4^{2-} and Mg^{2+} dominate the major solute composition of these aquifers (Fig. 4b). Karst springs are neutral to slightly alkaline with pH ranging from 7.01 to 8.13. Slightly higher pH (8.13) readings were observed in water samples from Ertefa spring, which is dominated by snowmelt water with low residence time. The water temperature of the springs ranged from 4.5 to $7.5 \text{ }^\circ\text{C}$. The lower temperatures were observed at the high discharge time, while temperature becomes $2\text{--}3 \text{ }^\circ\text{C}$ warmer in the base flow conditions. Based on the spring drainage type, hydrochemistry and EC, the springs are classified into two groups (Table 1). The first group includes the Abrizeh, Doberar, Ghezelkhani, Ertfa and Cheshmekhorni springs,

Table 1 Physico-chemical characteristics of the main karst springs in Lar watershed

Spring name	Sample ID in Figs. 5 and 9	Q (L/s)	T (°C)	EC (μ S/cm)	pH	Ca^{2+} (mg/L)	Mg^{2+} (mg/L)	Na^+ (mg/L)	K^+ (mg/L)	HCO_3^- (mg/L)	Cl^- (mg/L)	SO_4^{2-} (mg/L)	NO_3^- (mg/L)	TDS (mg/L)
Abrizeh	Ab-1	1,050	6	299	7.8	49.6	6.8	5.2	0.60	157	3.3	19.0	5.5	248
Abrizeh	Ab-2	120	5	275	7.9	32.1	6.3	4.9	0.60	134	4.2	18.6	4.4	205
Cheshmekhoni	Ch	500	7.5	269	7.9	44.4	5.2	5.4	0.40	134	2.8	26.1	5.4	224
Delichay ^a	D	2,500	5	478	7.2	68.0	18.2	10.0	4.30	255	18.2	83.6	3.5	461
Doberar	Do-1	2,100	7.5	360	7.8	69.0	9.3	5.5	0.60	199	4.1	22.5	5.8	316
Doberar	Do-2	1,850	5.6	345	7.0	54.7	9.3	6.3	0.60	178	4.6	23.3	5.3	282
Doberar	Do-3	1,400	5	372	7.9	50.6	9.0	6.3	0.60	197	5.1	22.6	4.7	296
Doberar	Do-4	1,300	5.3	375	7.9	63.7	8.6	6.1	0.61	208	5.3	22.1	5.5	320
Ertefa	E	160	4.5	159	8.1	50.0	1.1	0.7	0.32	153	0.7	3.3	5.0	215
Gezelkhani	Gh-1	456	5.5	280	7.9	50.7	5.2	1.4	0.51	128	2.5	6.5	9.2	204
Gezelkhani	Gh-2	320	5.5	279	7.9	50.4	5.4	1.5	0.52	132	2.8	6.4	8.8	208
Gezelkhani	Gh-3	185	6	287	7.9	50.3	5.9	1.6	0.51	139	2.9	7.0	8.9	216
Gezelkhani	Gh-4	155	7.5	272	7.9	47.4	6.1	1.7	0.52	139	3.5	6.8	8.3	214
Vararo ^a	V-1	1,050	7.1	850	7.7	77.8	22.5	10.0	1.90	206	16.7	38.0	5.2	376
Vararo ^a	V-2	450	7.2	608	7.7	81.0	22.0	10.0	2.01	201	17.8	35.0	5.4	361

^a Delichay and Vararo springs are classified as group 2, while the rest of the springs are group 1 (see section ‘Chemical composition of the main karst springs’)

characterized with higher quality ($150 < EC < 375 \mu$ S/cm) and relatively lower mineralization, while the second group (i.e. Vararo and Delichay) have higher EC ($478 < EC < 850 \mu$ S/cm) and higher ion concentrations. The values of TDS vary from 205 to 320 mg/L and 361 to 461 mg/L in the first and second groups, respectively. The chloride concentrations of the first group of springs are between 0.7 and 5.3 mg/L, while in the second group they vary between 16.7 and 18.2 mg/L. Similarly, the Na^+ concentration is lower in the first group (0.73–6.3 mg/L) and higher in the second group (~10 mg/L). Likewise, the Mg^{2+} concentrations follow the same trend, which range from 1.05 to 9.3 mg/L and 18.2 to 22.4 mg/L in the first and second groups. Sulfate

content varies between 3.3 and 83.6 mg/L with the highest amount in the second group of the springs. Nitrate concentrations in the vast majority of the springs vary between 2.6 and 5.5 mg/L with the exception of Ghezelkhani spring, which shows a higher concentration of nitrate with an average of 8.8 mg/L.

Stable isotope content of the main karst springs

For evaluation of the stable isotope content of the main karst springs in the Lar catchment, sampling was carried out at peak flow conditions and during recession periods. Based on discharge variation, 15 water samples out of the 35 samples from

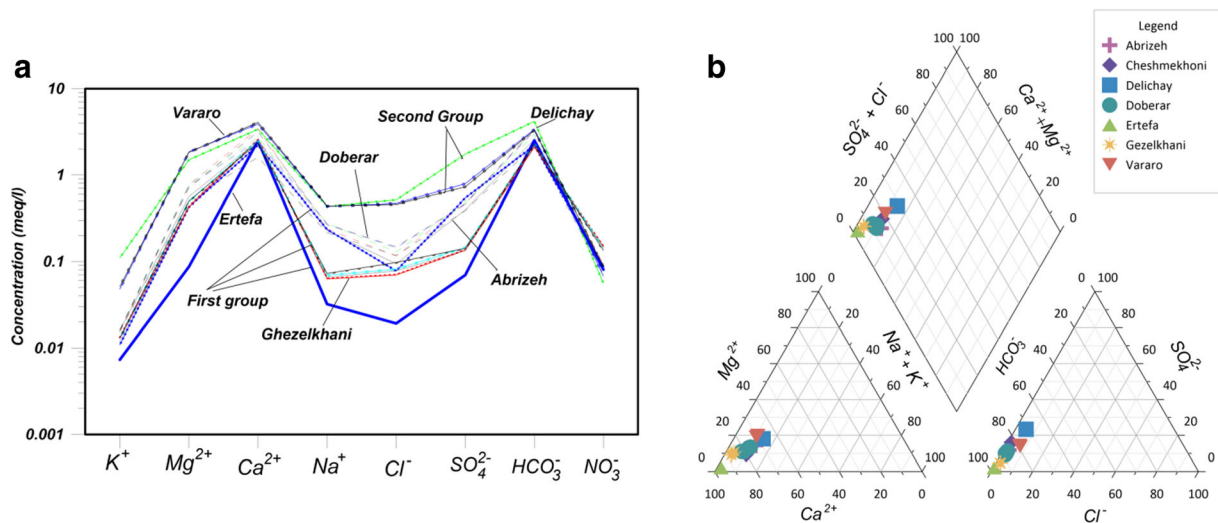


Fig. 4 a Schoeller diagram of the main karst spring samples, b Piper diagram showing the chemical composition of water samples in the study area

the main karst springs were selected for stable isotope analysis. The local meteoric water line (LMWL) of the study area, based on the values of the $\delta^{18}\text{O}$ and δD contents of rain and snow samples, is defined by the equation $\delta\text{D} = 7.7\delta^{18}\text{O} + 8.5$ (unpublished data). The stable isotope content of the precipitation samples varies from 0.88 to -15.9‰ (average value: -8.15‰) and 10.3 to -115‰ (average value: -53.9‰) for $\delta^{18}\text{O}$ and δD , respectively (Table 2). The results of stable isotope analysis of the karst springs of Lar catchment are summarized in Table 3 and displayed in Fig. 5a,b. The isotope composition of the spring water samples ranges from -7.09 to -8.97‰ and -43.6 to -53‰ for $\delta^{18}\text{O}$ and δD , respectively (Table 3). As shown in Fig. 5a, the isotope content of $\delta^{18}\text{O}$ and δD in precipitation (snow and rain) shows good agreement with the GMWL. The scatter plot of $\delta\text{D}-\delta^{18}\text{O}$ shows that the samples of the karst springs are clustered above both the GMWL and LMWL (Fig. 5a, b) following the liner regression of $\delta\text{D} = 4.34\delta^{18}\text{O} - 13.5$ ($R = 0.75$). The deuterium excess values were calculated as $\text{d-excess} = \delta\text{D} - 8\delta^{18}\text{O}$ (Dansgaard 1964). The d-excess of karst water samples ranges between 11.6 and 18.7‰ (Table 3).

Discussion

Geochemical evolution of karst waters

Figure 4a, b shows a Schoeller diagram and Piper plot of the main karst springs in Lar watershed. Based on hydrochemical

results, all samples are representing $\text{Ca}^{2+} - \text{HCO}_3^-$ and $\text{Ca}^{2+} - \text{Mg}^{2+} - \text{HCO}_3^-$ facies with dominance of HCO_3^- , Ca^{2+} and Mg^{2+} in decreasing order. Gibbs diagrams (Gibbs 1970) which depict log TDS against both the ratios of cations $\text{Na}^+ / (\text{Na}^+ + \text{Ca}^{2+})$ and the ratio of anions $\text{Cl}^- / (\text{Cl}^- + \text{HCO}_3^-)$ are widely used for understanding relative importance of the major natural controlling mechanisms of groundwater chemistry. The samples have been plotted in Gibbs diagrams and these show that all samples are clustered in the rock dominance zone (Fig. 6), supporting that the rock–water interaction is controlling the concentration of ions. Plotting the samples on Langelier-Ludwig (1942) diagrams indicates that spring water samples are characterized by the governance of carbonates dissolution (Fig. 7).

A scatter plot of Na^+ versus Cl^- was employed to identify the potential sources of Na^+ and Cl^- (Fig. 8a). As can be seen in Fig. 8, some of the spring samples plotted very close to or below the halite dissolution line (Ertefa, Vararo, Delichay and Ghezalkhani) and a few others plot above this line, which suggests excess Na^+ (Doberar, Abrizeh and Cheshmekhoni), possibly resulting from silicate weathering (Zhang et al. 2014). Likewise, the $\text{Na}^+ / \text{Cl}^-$ ratio greater than 1 indicates either the presence of silicate weathering or ion exchange between Na^+ and Ca^{2+} . The significant increase of Na^+ content in the karst water (Abrizeh, Doberar and Cheshmekhoni) is possibly originating from silicate weathering of patchy tuff outcrop in the catchment area of these springs (e.g., feldspars).

The plot of $(\text{Ca}^{2+} + \text{Mg}^{2+})$ vs. HCO_3^- (Fig. 8b) shows that data points deviate slightly above the 1:1 line, indicating that

Table 2 Isotopic composition of precipitation (*P*) at the nearest stations from August 2015 to July 2016 (unpublished data)

Sample ID	Elevation (m a.s.l.)	Precipitation type	Date	<i>P</i> (mm)	δD (‰)	$\delta^{18}\text{O}$ (‰)	<i>T</i> (°C)	d-excess (‰)
Druk-2015/01	2,670	Rain	9/17/2015	23.0	8.12	-0.62	15.00	13.08
Druk-2015/02	2,670	Rain	10/18/2015	15.6	-25.82	-3.55	12.70	2.58
Druk-2015/03	2,850	Snowpack	11/8/2015	50.2	-54.89	-8.45	-2.79	12.71
Druk-2015/04	2,830	Fresh snow	12/1/2015	53.5	-109.88	-15.06	-7.18	10.60
Druk-2016/05	2,667	Snowpack	1/16/2016	80.0	-54.07	-8.72	-6.54	15.69
Druk-2016/05-1	2,670	Snowpack	4/6/2016	105.0	-37.67	-6.63	-2.91	15.37
Druk-2016/06	2,667	Snowpack	2/12/2016	45.0	-73.38	-10.98	-3.00	14.46
Druk-2016/07	2,667	Snowpack	3/7/2016	46.0	-79.00	-11.70	8.20	14.60
Druk-2016/08	2,667	Fresh snow	4/6/2016	4.8	-110.37	-14.93	12.06	9.05
Druk-2016 /09	2,670	Rain	5/10/2016	76.0	-19.82	-3.86	17.56	11.06
Lehra-2015/02	2,950	Rain	10/18/2015	15.6	-20.45	-2.08	12.70	-3.81
Lehra-2015/03	3,000	Snowpack	11/8/2015	53.0	-55.98	-9.00	-2.79	16.02
Lehra-2015/04	3,000	Fresh snow	12/1/2015	55.3	-115.50	-15.90	-7.18	11.70
Lehra-2016/05	3,000	Snowpack	1/16/2016	82.0	-44.32	-7.80	-6.54	18.08
Lehra-2016/06	3,000	Snowpack	2/12/2016	48.0	-48.05	-8.12	-2.91	16.91
Lehra-2016/07	3,000	Snowpack	3/7/2016	48.0	-93.44	-12.49	3.58	6.48
Lehra-2016/08	2,900	Snowpack	4/6/2016	112.0	-36.72	-6.22	8.20	13.04
Lehra-2016 /09	2,950	Rain	5/10/2016	79.0	-28.84	-4.94	12.06	10.68
Lehra-2016/10	2,950	Rain	6/15/2016	35.0	-35.83	-6.24	17.56	14.09

Table 3 Stable isotope content of the main karst springs in Lar watershed

Spring name	Sample ID in Figs. 5 and 9	Sampling date	Discharge elevation (m a.s.l.)	Q (L/s)	$\delta^{18}\text{O}$ (‰)	δD (‰)	d-excess (‰)	AECH ^a (m a.s.l.)
Abrizeh	Ab-1	07/22/2015	2,648	1,050	-7.65	-47.1	14.12	3,250
Abrizeh	Ab-2	08/23/2015	2,648	120	-7.55	-46.8	13.57	3,250
Cheshmekhoni	Ch	09/18/2015	2,640	500	-8.02	-47.3	16.89	2,750
Delichay	D	06/20/2015	2,973	2,500	-8.37	-52.2	14.78	3,400
Doberar	Do-1	09/18/2015	2,647	2,100	-8.45	-49.8	17.80	3,300
Doberar	Do-2	06/20/2015	2,647	1,850	-7.26	-46.5	11.64	3,300
Doberar	Do-3	07/23/2015	2,647	1,400	-8.16	-48.2	17.13	3,300
Doberar	Do-4	10/23/2015	2,647	1,300	-7.91	-46.3	16.99	3,300
Ertefa	E	06/20/2015	3,250	160	-7.49	-44.6	15.3	3,650
Gezelkhani	Gh-1	06/20/2015	2,556	456	-7.31	-45.6	12.86	2,850
Gezelkhani	Gh-2	07/23/2015	2,556	320	-8.01	-47.2	16.9	2,850
Gezelkhani	Gh-3	08/25/2015	2,556	185	-7.09	-43.9	13.14	2,850
Gezelkhani	Gh-4	09/18/2015	2,556	155	-7.95	-47.6	16.04	2,850
Vararo	V-1	06/17/2015	2,746	1,050	-7.86	-50.1	12.78	3,200
Vararo	V-2	09/18/2015	2,746	450	-8.97	-53.0	18.785	3,200

^a Average elevation of catchment area

the carbonate weathering itself is not sufficient to explain these ion concentrations. Therefore, another source should be responsible for the excess amount of calcium and magnesium. Binary plots of $(\text{Ca}^{2+} + \text{Mg}^{2+})$ versus $(\text{SO}_4^{2-} + \text{HCO}_3^-)$; Fig. 8c show that most of the samples fall around the 1:1 line which indicates that dissolution of calcite, dolomite and gypsum are the dominant reactions in the system (Zaidi et al. 2015). Extra amounts of $\text{Ca}^{2+} + \text{Mg}^{2+}$ over $\text{SO}_4^{2-} + \text{HCO}_3^-$ indicate the presence of ion exchange, while excess amounts of $\text{SO}_4^{2-} + \text{HCO}_3^-$ over $\text{Ca}^{2+} + \text{Mg}^{2+}$ show occurrence of reverse ion exchange (Hounslow 1995; Fisher and Mulican 1997; Krishnaraj et al. 2011; Zaidi

et al. 2015). The samples of Ghezelkhani, Vararo and Delichay springs show deviation from this line indicating the presence of ion exchange, rivers ion exchange (Rajmohan and Elango 2004) or mixing. An excess of calcium and magnesium over $\text{SO}_4^{2-} + \text{HCO}_3^-$ in Ghezelkhani and Vararo springs may be due to exchange of sodium in water by calcium and magnesium in the clay material. Enrichment of Na^+ , Mg^{2+} and SO_4^{2-} in Doberar, Cheshmekhoni and Abrizeh water samples with linear correlation of the SO_4^{2-} and Na^+ (Fig. 8d) indicates weathering and dissolution of mirabilite and Mg^{2+} bearing sulfate minerals (Zhou et al. 2016), which could be related to the

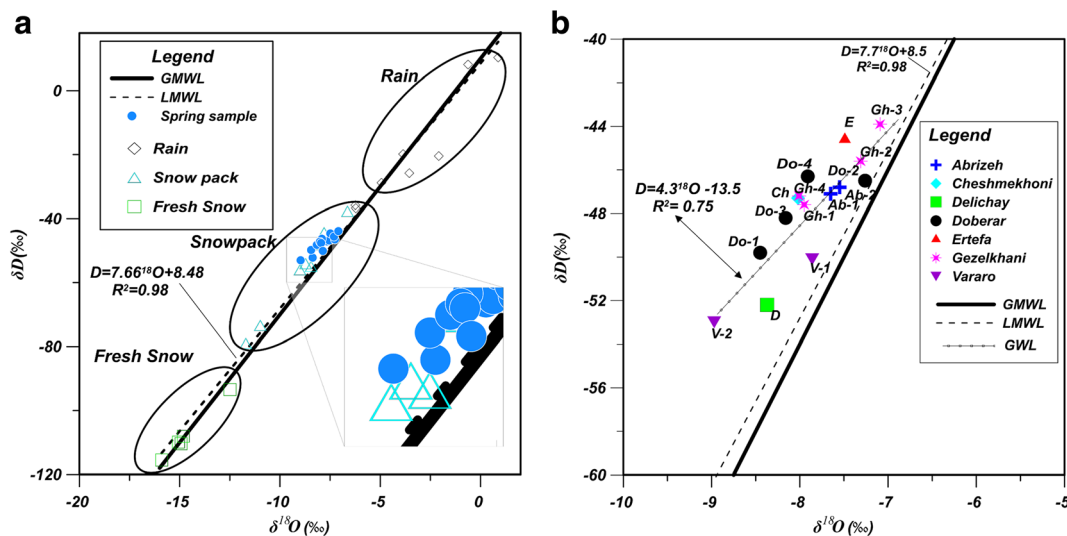


Fig. 5 **a** The relationship between δD and $\delta^{18}\text{O}$ in precipitation and the main karst springs with the global and local meteoric water lines (GMWL and LMWL), and **b** a close view of the isotope composition and regression line of the karst springs isotope contents in Lar watershed

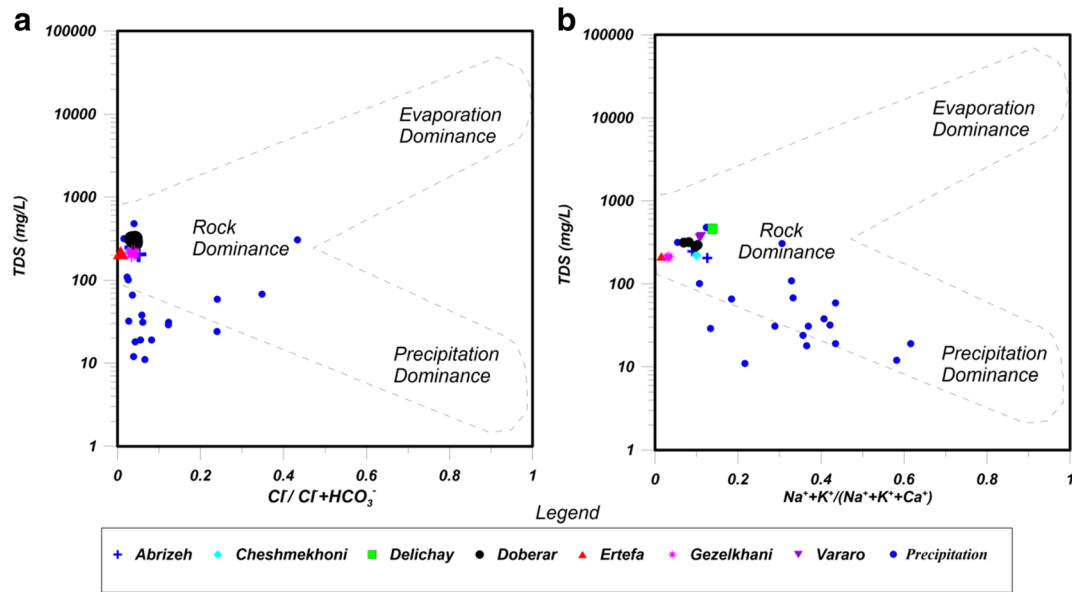


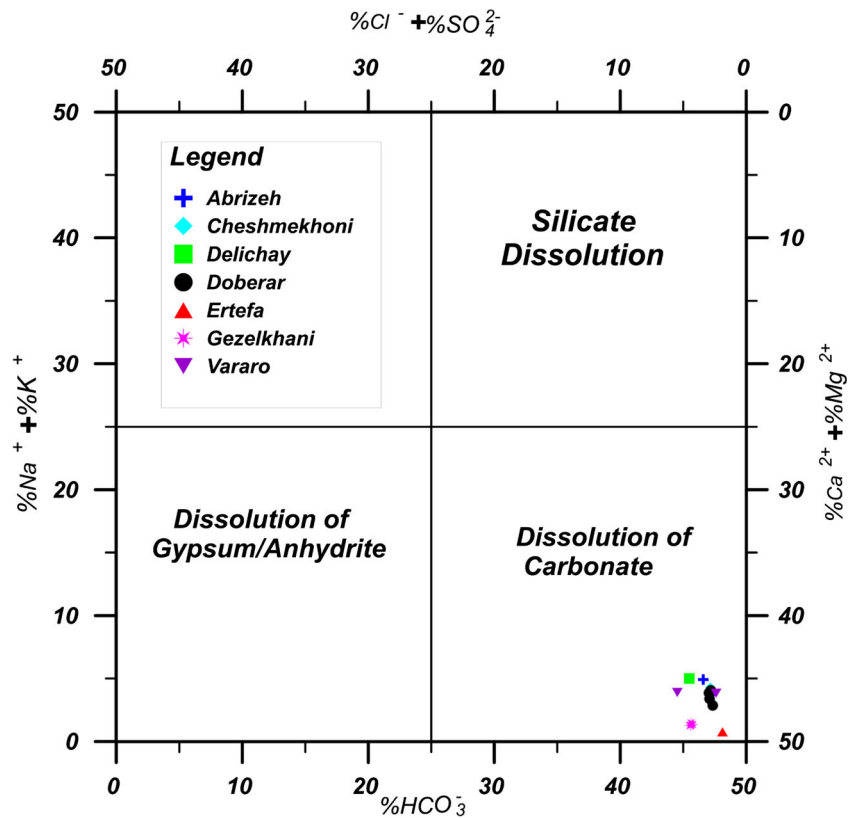
Fig. 6 Gibbs diagrams of the main karst spring samples of Lar watershed. TDS vs. **a** $Cl^- / (Cl^- + HCO_3^-)$, and **b** $Na^+ / (Na^+ + Ca^{2+})$

partially overlying tuff over the carbonate formations in the catchment areas of the springs.

Low concentration of Mg^{2+} indicates that calcite dissolution is mainly controlling chemical composition of the spring's water, with scarce dolomite dissolution; however, elevated Mg^{2+} and HCO_3^- concentrations during low flow conditions (late summer and early autumn), when the spring water

is principally fed by the saturated zone of the aquifer (with higher residence time), while the chemical facies of the water remained calcium bicarbonate. The highest concentrations of NO_3^- were observed in the samples of Ghezelkhani spring, probably due to more intense and longer period of grazing by sheep. Generally, the physico-chemical results of the main karst spring samples showed that the karst aquifers in the

Fig. 7 Langelier-Ludwig plot of the karst spring samples



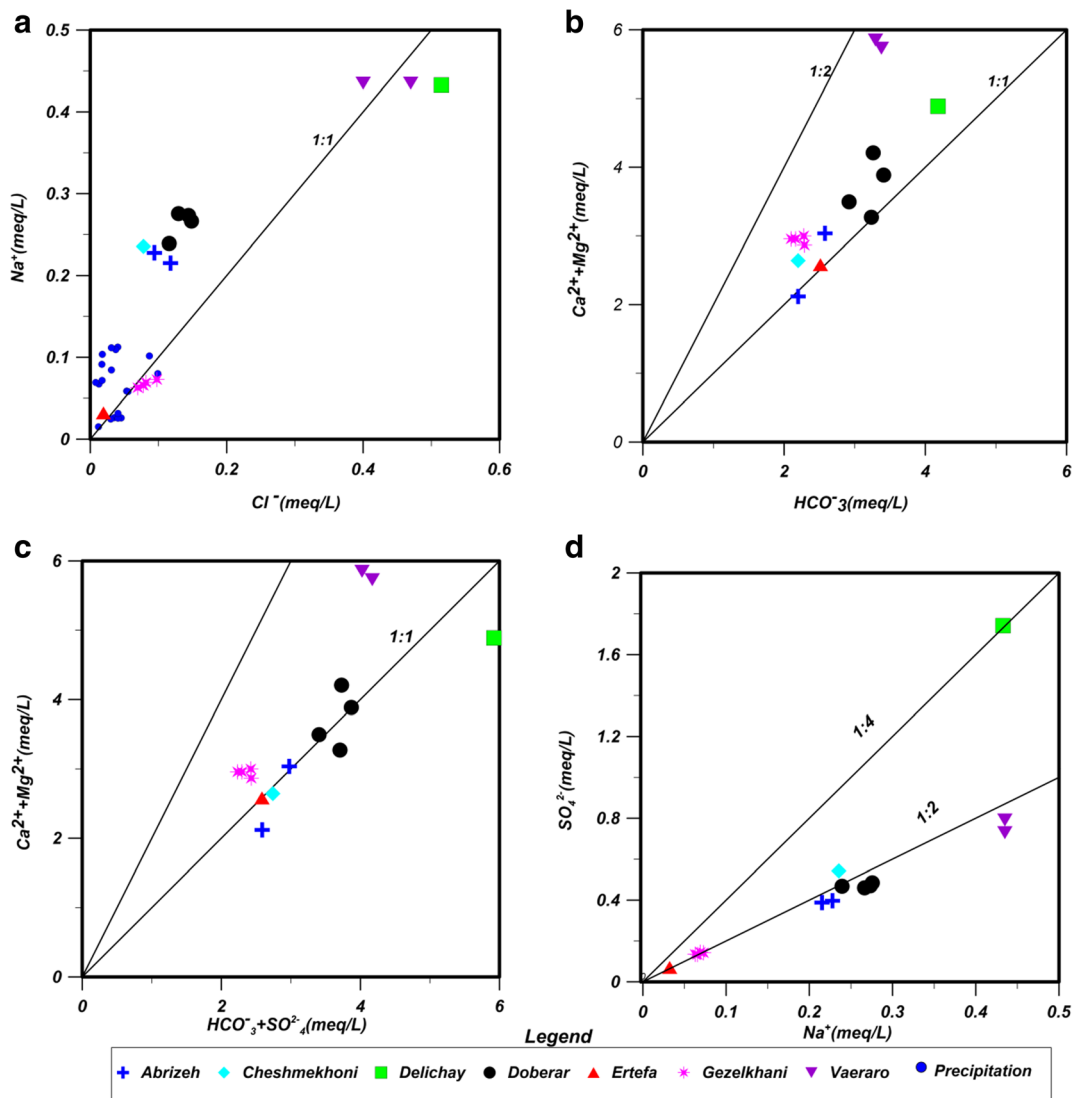


Fig. 8 Scatter plot of **a** Cl^- vs. Na^+ , **b** $\text{Ca}^{2+} + \text{Mg}^{2+}$ vs. HCO_3^- , **c** $\text{Ca}^{2+} + \text{Mg}^{2+}$ vs. $\text{SO}_4^{2-} + \text{HCO}_3^-$ and **d** Na^+ vs. SO_4^{2-} for the spring samples

study area situated far from Damavand volcano have higher quality than those in its vicinity.

Stable isotopes evolution of karst springs

The isotope composition of spring water samples shows little spatial variability, ranging from -7.09 to -8.97‰ and -43.8 to 52.9‰ for $\delta^{18}\text{O}$ and δD , respectively (Table 3) due to the diversity of catchment characteristics (geomorphology, elevation) and time of recharge, as the early melting recharge waters have lighter isotope content (Liu et al. 2008). Clustering of samples above both the GMWL and LMWL (Fig. 5a, b) reveals the effect of the moisture recycling by continental vapor (Fan et al. 2016). The low slope of the regression line (4.34) for the spring-water samples' isotope content and positioning above both the GMWL and LMWL are consistent with the evaporative slope of between 4 and 6 for semi-arid areas (Clark and

Fritz 1997; Kazemi et al. 2015). Likewise, the lower interception of the regression line (-13.5) indicates the presence of an evaporation effect before recharge (Thilakerathne et al. 2015; Wu et al. 2015). The isotope signatures of the spring water are close to the isotope content of the snow-pack samples, proposing that governance of recharge to the karst aquifers is by the snowmelt water (Pang et al. 2011).

The variation amplitude of isotope composition in precipitation is considerably larger than that in the spring waters (Fig. 5a). This suggests that there is an adjusting effect associated with the unsaturated zone and the low amount of rainfall is being lost through evapotranspiration. Further, snow preservation for longer periods makes it possible for snow-pack isotope content to affect post-deposition processes (Town et al. 2008). Since recharge is so fast in karst aquifers with small soil thickness, the evolution of the isotope content most probably occurs before the infiltration, during the period of accumulation of snow. This could be attributed to a post-

deposition effect on snow by air ventilation, which is the most important post-deposition parameter (Town et al. 2008).

Figure (9a) shows the temporal distribution of δD and $\delta^{18}O$ in two spring (Ghezelkhani and Doberar) for the sampling period from June 2015 to October 2015. Generally, both springs have depletion trends for the sampling period with shorter-term variations for δ^2H and $\delta^{18}O$ (Fig. 9a). Irregularity of δ^2H and $\delta^{18}O$ content for these two karst springs results from summer recharge events with enriched isotopic ratios. The more depleted isotope content in the base flow condition is ascribed to the diffuse recharge with early melt water as explained by Meeks and Hunkeler (2015). The higher variability of the isotope signature and chemical composition in Doberar karst spring, in comparison to the Ghezelkhani spring, is ascribed to the higher karstification as well as the timing and the quantity of the input to the system. The isotope ratio of $\delta^{18}O$ shows no significant correlation with elevation (Fig 9b); this indicates that rather than elevation, other

parameters (e.g., post deposition and rain on snow) is affecting the isotope content of the karst springs (Liu et al. 2008). All in all, the spring outlets with higher average elevation within their catchment area and with more snowfall in the catchment area exhibited the more depleted isotope composition.

Similarity between the d-excess values of karst water samples and snow samples signifies that the dominance of recharge from the snowmelt outweighs the recharge from rainfall. The mean value of d-excess for spring water samples is 15.3‰, which also indicates that the Lar watershed springs are recharged predominantly by the Mediterranean originated atmospheric water vapor in the cold season. It is worth mentioning that Abrizeh karst spring dries out in the early autumn and starts flowing again after 2 months due to early melting or rain events in early autumn that proves the springs water originated from recent precipitations, thus indicating the effect of recent precipitation events on flow

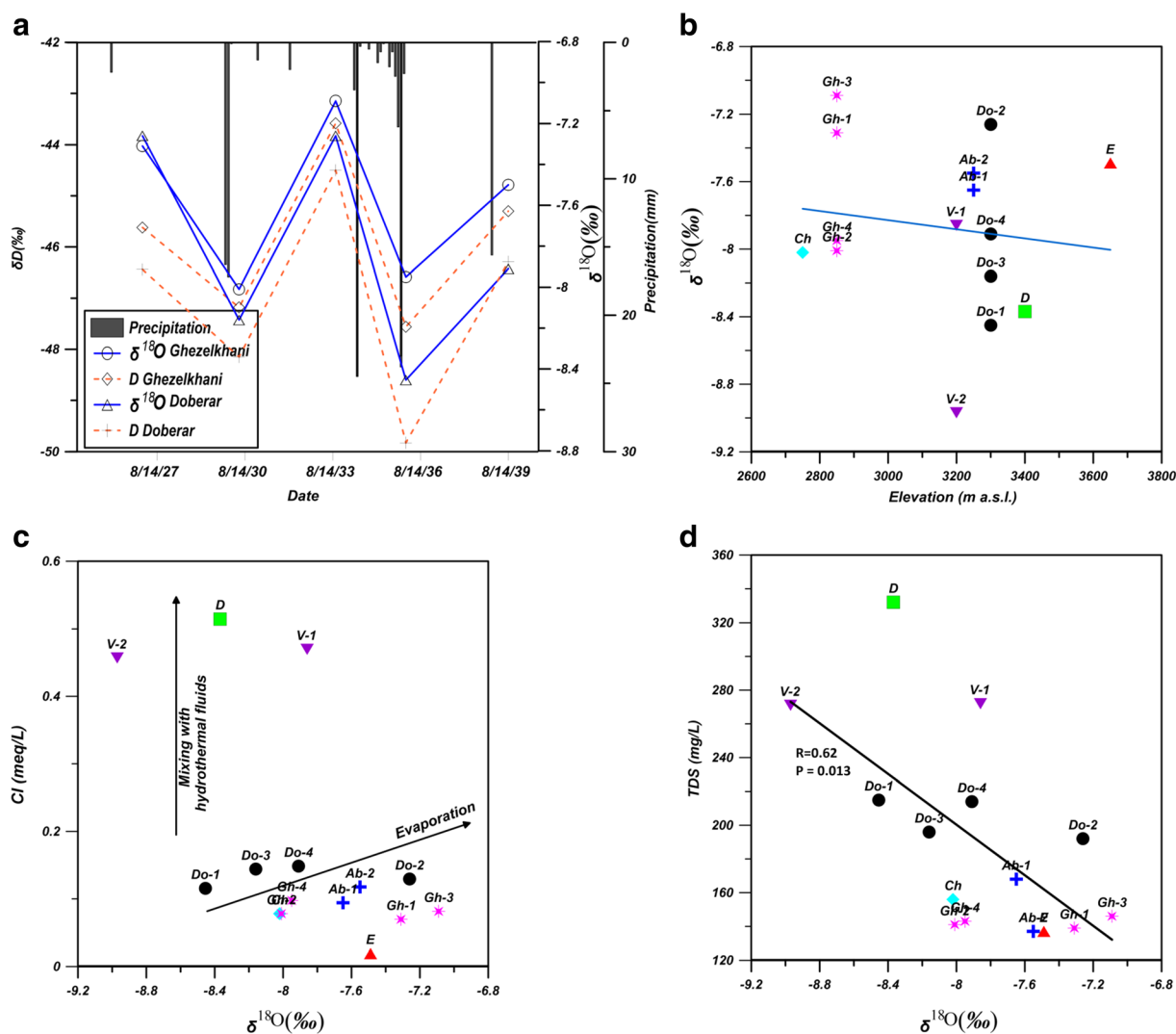


Fig. 9 a Temporal variation of the isotope content in two springs, b relationship between δD and average elevation of the spring catchments, c $\delta^{18}O$ vs. chloride concentrations, d relationship between $\delta^{18}O$ and average elevation of the spring catchments

regimes in the karst areas. The karst aquifers in the study area are higher in elevation compared with the neighbor landscapes, which makes it impossible for underground flow to contribute to these aquifers. Beside, there is no surface flow to the area, so that precipitation is the only possible recharge source. The similarity of the stable isotopes and d-excess values of the karst water and snowpack samples confirms that the recharge is from the snowmelt water.

The $\delta^{18}\text{O}$ versus chloride concentration plot (Fig 9c) indicates that the higher chloride in Vararo and Delichay springs originates from the mixing with hydrothermal fluids (Hernández-Antonio et al. 2015), while the other springs do not show such effects. The occurrence of a few small hot springs in the northeast of the study area confirms this hypothesis and also the occurrence of mixing with hydrothermal fluids. Likewise, the higher SO_4^{2-} concentrations in the second group of springs (Delichay and Vararo) most probably is due to sulfate emission from the deep faults associated with Damavand volcano. Generally, all of the ions except the nitrate show negative correlation with isotope ratios (Table 4). Correlation coefficients between δD and ions is higher than $\delta^{18}\text{O}$. To represent the ions concentration against isotope ratio the TDS vs. $\delta^{18}\text{O}$ depicted in Fig. 9d. As shown, more depleted isotope ratios have lower TDS concentration and vice versa, which may imply that the recharge type and longer residence time have an effect. Diffuse recharge occurs over the whole of the catchment area and recharge water travels along longer flow paths that lead to increasing residence time and more rock–water interactions. Thus, discharging water in base flow conditions shows higher ion concentrations and lighter isotope signatures.

Conclusions

This research examined the isotope content and hydrochemistry of the karst springs in the Lar watershed. The hydrochemistry compositions of the karst springs are characterized by $\text{Ca}^{2+} - \text{Mg}^{2+} - \text{HCO}_3^-$ type. The chemical composition of the main karst springs is controlled mainly by local geology and the water–rock interactions of limestone; however, the role of thermal fluids or emissions from the Damavand Volcano is significant for the second group of springs. Even though the discharging springs originate from the same formation with almost the same recharge sources (precipitation), mineralization of water in the free-draining springs Delichay and Vararo are considerably higher than overflow springs (Doberar, Ghezelkhani, Abrizeh, Cheshme Ertefa). Elevated ion concentrations in the second group of springs, in comparison to the first group, may be due to mixing with hydrothermal fluid, relatively longer residence time and flow at the bottom of the karstic aquifers in contact with the shale bedrock.

Based on the geological framework and isotope results, it could be concluded that the karst springs are mainly recharged by precipitation on the exposed carbonate rocks. The isotopic content of the main karst springs is very close to the isotopic content of the snowpack samples, with average d-excess of 15.3‰, which suggests that the recharge to the karst aquifers in the study area is predominantly supplied by snowmelt water that accumulates during the cold season. However, a high amount precipitation in the dry season can recharge the aquifers and affect the isotope content of the karst system. Generally, isotope content becomes depleted in the base flow, which indicates the presence of diffuse recharge during the cold season. Negative correlation of ion concentrations with isotope ratios

Table 4 Correlation coefficients among the major ions and stable isotopes

	EC	pH	Ca^{2+}	Mg^{2+}	Na^+	K^+	HCO_3^-	Cl^-	SO_4^{2-}	NO_3^-	TDS	$\delta^{18}\text{O}$	δD
EC	1.00												
pH	−0.35	1.00											
Ca^{2+}	0.80 ^a	−0.35	1.00										
Mg^{2+}	0.94 ^a	−0.49	0.83 ^a	1.00									
Na^+	0.81 ^a	−0.56 ^b	0.68 ^a	0.89 ^a	1.00								
K^+	0.59 ^b	−0.57 ^b	0.58 ^b	0.76 ^a	0.71 ^a	1.00							
HCO_3^-	0.63 ^b	−0.53 ^b	0.76 ^a	0.74 ^a	0.82 ^a	0.73 ^a	1.00						
Cl^-	0.86 ^a	−0.49	0.77 ^a	0.96 ^a	0.86 ^a	0.88 ^a	0.75 ^a	1.00					
SO_4^{2-}	0.57 ^b	−0.64 ^a	0.53 ^b	0.73 ^a	0.83 ^a	0.93 ^a	0.81 ^a	0.82 ^a	1.00				
NO_3^-	−0.31	0.36	−0.23	−0.40	−0.70 ^a	−0.45	−0.64 ^a	−0.45	−0.64 ^a	1.00			
TDS	0.75 ^a	−0.58 ^b	0.81 ^a	0.85 ^a	0.88 ^a	0.85 ^a	0.96 ^a	0.87 ^a	0.89 ^a	−0.59 ^b	1.00		
$\delta^{18}\text{O}$	−0.44	0.06	−0.60 ^b	−.58 ^b	−0.59 ^b	−0.48	−0.56 ^b	−0.59 ^b	−0.51	0.36	−0.60 ^b	1.00	
δD	−0.70 ^a	0.41	−0.71 ^a	−.85 ^a	−0.82 ^a	−0.75 ^a	−0.70 ^a	−0.85 ^a	−0.76 ^a	0.47	−0.80 ^a	0.87 ^a	1.00

^a Correlation is significant at the 0.01 level (two-tailed)

^b Correlation is significant at the 0.05 level (two-tailed)

confirms the presence of wintertime diffuse recharge with a depleted isotope signature and longer residence time.

References

- Alavi M (1996) Tectonostratigraphic synthesis and structural style of the Alborz mountain system in northern Iran. *J Geodyn* 21(1):1–33. [https://doi.org/10.1016/0264-3707\(95\)00009-7](https://doi.org/10.1016/0264-3707(95)00009-7)
- Andreo B, Carrasco F, Bakalowicz M, Mudry J, Vadillo I (2002) Use of the hydrodynamic and hydrochemistry to characterise carbonate aquifers: case study of the Blanca-Mijas unit (Malaga, southern Spain). *Environ Geol* 43:108–119. <https://doi.org/10.1007/s00254-002-0614-z>
- Bhat NA, Jeelani GH (2015) Delineation of the recharge areas and distinguishing the sources of karst springs in Bringi watershed, Kashmir Himalayas using hydrochemistry and environmental isotopes. *J Earth Syst Sci* 124(8):1667–1676. <https://doi.org/10.1007/s12040-015-0629-y>
- Birk S, Liedl R, Sauter M (2004) Identification of localised recharge and conduit flow by combined analysis of hydraulic and physico-chemical spring responses (Urenbrunnen, SW-Germany). *J Hydrol* 286(1–4):179–193. <https://doi.org/10.1016/j.jhydrol.2003.09.007>
- Blasch KW, Bryson JR (2007) Distinguishing sources of ground water recharge by using delta2H and delta18O. *Ground Water* 45(3):294–308. <https://doi.org/10.1111/j.1745-6584.2006.00289.x>
- Clark ID, Fritz P (1997) Environmental isotopes in hydrogeology. CRC, Boca Raton
- Dansgaard W (1964) Stable isotopes in precipitation. *Tellus* 16:436–469
- Davidson J, Hassanzadeh J, Berzins R, Stockli DF, Bashukooh B, Turrin B, Pandamouz A (2004) The geology of Damavand volcano, Alborz Mountains, northern Iran. *Geol Soc Am Bull* 116(1):16. <https://doi.org/10.1130/B25344.1>
- Doctor DH, Alexander EC Jr (2005) Interpretation of water chemistry and stable isotope data from a karst aquifer according to flow regimes identified through hydrograph recession analysis. Proceedings US Geological Survey Karst Interest Group, Rapid City, SD, US Geological Survey, Reston, VA, pp 82–92
- Doctor DH, Alexander EC, Petrič M, Kogovšek J, Urbanc J, Lojen S, Stichler W (2006) Quantification of karst aquifer discharge components during storm events through end-member mixing analysis using natural chemistry and stable isotopes as tracers. *Hydrogeol J* 14(7):1171–1191. <https://doi.org/10.1007/s10040-006-0031-6>
- Dursun OF, Celiker M, Firat M (2016) Hydrological properties of the Derme Karstic Springs by using hydrogeochemical analyses and environmental isotope techniques. *CLEAN Soil Air Water* 44(2):143–153. <https://doi.org/10.1002/clen.201400035>
- Fan Y, Chen Y, He Q, Li W, Wang Y (2016) Isotopic characterization of river waters and water source identification in an inland river, Central Asia. *Water* 8(7):286. <https://doi.org/10.3390/w8070286>
- Fiorillo F (2014) The recession of spring hydrographs, focused on karst aquifers. *Water Resour Manag* 28:1781–1805. <https://doi.org/10.1007/s11269-014-0597-z>
- Fisher RS, Mulican WF (1997) Hydrochemical evolution of sodium-sulfate and sodium-chloride groundwater beneath the northern Chihuahuan Desert, Trans-Pecos, Texas, USA. *Hydrogeol J* 10(4):455–474
- Ford DC, Williams PW (2007) Karst hydrogeology and geomorphology. Wiley, Chichester, UK, 562 pp
- Fu T, Chen H, Zhang W, Nie Y, Gao P, Wang K (2015) Spatial variability of surface soil saturated hydraulic conductivity in a small karst catchment of Southwest China. *Environ Earth Sci* 74(3):2381–2391. <https://doi.org/10.1007/s12665-015-4238-5>
- Gibbs JR (1970) Mechanisms Controlling World Water Chemistry. *Science* 170 (3962):1088–1090
- Hamdan I, Wiegand B, Toll M, Sauter M (2016) Spring response to precipitation events using $\delta^{18}\text{O}$ and $\delta^2\text{H}$ in the Tanour catchment, NW Jordan. *Isot Environ Health Stud* 52(6):682–693. <https://doi.org/10.1080/10256016.2016.1159205>
- Hatipoglu-Bagci Z, Sazan MS (2014) Characteristics of karst springs in Aydıncık (Mersin, Turkey), based on recession curves and hydrochemical and isotopic parameters. *Q J Eng Geol Hydrogeol* 47(1):89–99. <https://doi.org/10.1144/qjegh2013-074>
- Hernández-Antonio A, Mählknecht J, Tamez-Meléndez C, Ramos-Leal J, Ramírez-Orozco A, Parra R, et al (2015) Groundwater flow processes and mixing in active volcanic systems: the case of Guadalajara (Mexico). *Hydrol Earth Syst Sci* 19(9):3937–3950. <https://doi.org/10.5194/hess-19-3937-2015>
- Hounslow AW (1995) Water quality data: analysis and interpretation. Oklahoma State University, Stillwater, 397 pp
- Jukić D, Denić-Jukić V (2015) Investigating relationships between rainfall and karst-spring discharge by higher-order partial correlation functions. *J Hydrol* 530:24–36. <https://doi.org/10.1016/j.jhydrol.2015.09.045>
- Kanduč T, Mori N, Kocman D, Stibilj V, Grassa F (2012) Hydrogeochemistry of alpine springs from North Slovenia: insights from stable isotopes. *Chem Geol* 300–301:40–54. <https://doi.org/10.1016/j.chemgeo.2012.01.012>
- Kazemi R (2003) Reconnaissance of karsts hydrology in the Lar catchments, Iran using Rs and GIS, MSc Thesis. ITC, Enschede, The Netherlands, 48 pp
- Kazemi GA, Ichianagi K, Shimada J (2015) Isotopic characteristics, chemical composition and salinization of atmospheric precipitation in Shahrood, northeastern Iran. *Environmental Earth Sciences*, 73(1), 361–374. <https://doi.org/10.1007/s12665-014-3430-3>
- Klaus J, McDonnell JJ (2013) Hydrograph separation using stable isotopes: review and evaluation. *J Hydrol* 505:47–64. <https://doi.org/10.1016/j.jhydrol.2013.09.006>
- Krishnaraj S, Murugesan V, Vijayaraghavan K, Sabarathinam C, Paluchamy A, Ramachandran M (2011) Use of hydrochemistry and stable isotopes as tools for groundwater evolution and contamination investigations. *Geosciences*, 1(1), 16–25. <https://doi.org/10.5923/j.geo.20110101.02>
- Kohfahl C, Rodriguez M, Fenk C, Menz C, Benavente J, Hubberten H, Meyer H, Paul L, Knappe A, López-Geta JA, Pekdeger A (2008) Characterising flow regime and interrelation between surface-water and ground-water in the Fuente de Piedra salt lake basin by means of stable isotopes, hydrogeochemical and hydraulic data. *J Hydrol* 351(1–2):170–187. <https://doi.org/10.1016/j.jhydrol.2007.12.008>
- Langelier WF, Ludwig HF (1942) Graphical method for indicating of the mineral character of natural waters. *J. Am. W.W. Assn.* 34, 335–352
- Larsen D, Swihart GH, Xiao Y (2001) Hydrochemistry and isotope composition of springs in the Tecopa basin, southeastern California, USA. *Chem Geol* 179:17–35. [https://doi.org/10.1016/s0009-2541\(01\)00313-8](https://doi.org/10.1016/s0009-2541(01)00313-8)
- Liu Y, An S, XuZ FN, Cui J, Wang Z, Liu S, Pan J, Lin G (2008) Spatio-temporal variation of stable isotopes of river waters, water source identification and water security in the Heishui Valley (China) during the dry-season. *Hydrogeol J* 16(2):311–319. <https://doi.org/10.1007/s10040-007-0260-3>
- Malik P (2015) Evaluating discharge regimes of karst aquifer. In: Stevanović Z (ed) Karst aquifer: characterization and engineering. Series: Professional Practice in Earth Science. Springer, Cham, pp 205–249
- Meeks J, Hunkeler D (2015) Snowmelt infiltration and storage within a karstic environment, Vers Chez le Brandt, Switzerland. *J Hydrol* 529:11–21. <https://doi.org/10.1016/j.jhydrol.2015.06.040>
- Miao J, Liu G, Cao B, Hao Y, Chen J, Yeh TCJ (2014) Identification of strong karst groundwater runoff belt by cross wavelet transform.

- Water Resour Manag 28(10):2903–2916. <https://doi.org/10.1007/s11269-014-0645-8>
- Padilla A, Pulido-Bosch A, Mangin A (1994) Relative importance of Baseflow and Quickflow from hydrographs of karst spring. *Ground Water* 32(2):267–277. <https://doi.org/10.1111/j.1745-6584.1994.tb00641.x>
- Pang Z, Kong Y, Froehlich K, Huang T, Yuan L, Li Z, Wang F (2011) Processes affecting isotopes in precipitation of an arid region. *Tellus B: Chem Phys Meteorol* 63(3):352–359. <https://doi.org/10.1111/j.1600-0889.2011.00532.x>
- Piper AM (1944) A graphic procedure in the geochemical interpretation of water analyses. *Trans Am Geophys Union* 6:914–923
- Poulain A, Rochez G, Bonniver I, Hallet V (2015) Stalactite drip-water monitoring and tracer tests approach to assess hydrogeologic behavior of karst vadose zone: case study of Han-Sur-Lesse (Belgium). *Environ Earth Sci* 74(12):7685–7697. <https://doi.org/10.1007/s12665-015-4696-9>
- Pu T, He Y, Zhang T, Wu J, Zhu G, Chang L (2013) Isotopic and geochemical evolution of ground and river waters in a karst dominated geological setting: a case study from Lijiang basin, South-Asia monsoon region. *Appl Geochem* 33:199–212. <https://doi.org/10.1016/j.apgeochem.2013.02.013>
- Raeisi E, Karami GH (1996) The governing factors of the physical and hydrochemical characteristics of karst springs. *Carbon Evap* 2(2):162–168
- Raghavendra NS, Deka PC (2015) Sustainable development and management of groundwater resources in mining affected areas: a review. *Proc Earth Planet Sci* 11:598–604. <https://doi.org/10.1016/j.proeps.2015.06.061>
- Rajmohan N, Elango L (2004) Identification and evolution of hydrogeochemical processes in the groundwater environment in an area of the Palar and Cheyyar river basins, southern India. *Environ Geol* 46(1):47–61. <https://doi.org/10.1007/s00254-004-1012-5>
- Seeyan S, Merkel B (2014) Determination of recharge by means of isotopes and water chemistry in Shaqlawa-Harrir Basin, Kurdistan region, Iraq. *Hydrol Curr Res* 5:179. <https://doi.org/10.4172/2157-7587.1000179>
- Shabanian E, Acocella V, Gioncada A, Ghasemi H, Bellier O (2012) Structural control on volcanism in interpolate post collisional settings: Late Cenozoic to Quaternary examples of Iran and eastern Turkey. *Tectonics* 31(3), TC3013
- Stevanovic Z (2015) Budget and general assessment of Karst groundwater resources. In: Stevanovic Z (ed) *Karst aquifers characterization and engineering*. Series: Professional Practice in Earth Science. Springer, Cham, Switzerland, pp 171–2001
- Stocklin J (1968) Structural history and tectonics of Iran: a review. *AAPG Bull* 52(7):1229–1258
- Tang R, Shu L, Lu C, Zhang C, Fan J, Appiah-Adjei EK (2015) Laboratory analog analysis of spring recession curve in a karst aquifer with fracture and conduit domains. *J Hydrol Eng* 21(2):0601501–06015013–13. [https://doi.org/10.1061/\(ASCE\)HE.1943-5584.0001271](https://doi.org/10.1061/(ASCE)HE.1943-5584.0001271)
- Thilakerathne A, Schüth C, Chandrajith R (2015) The impact of hydrogeological settings on geochemical evolution of groundwater in karstified limestone aquifer basin in Northwest Sri Lanka. *Environ Earth Sci* 73(12):8061–8073. <https://doi.org/10.1007/s12665-014-3962-6>
- Town MS, Warren SG, Walden VP, Waddington ED (2008) Effect of atmospheric water vapor on modification of stable isotopes in near-surface snow on ice sheets. *J Geophys Res Atmos* 113(D24). <https://doi.org/10.1029/2008JD009852>
- Turk J, Malard A, Jeannin PY, Petrič M, Gabrovšek F, Ravbar N, Vouillamoz J, Slabe T, Sordet V (2015) Hydrogeological characterization of groundwater storage and drainage in an alpine karst aquifer (the Kanin Massif, Julian Alps). *Hydrol Process* 29(8):1986–1998. <https://doi.org/10.1002/hyp.10313>
- Wu H, Zhang X, Xiaoyan L, Li G, Huang Y (2015) Seasonal variations of deuterium and oxygen-18 isotopes and their response to moisture source for precipitation events in the subtropical monsoon region. *Hydrol Process* 29(1):90–102. <https://doi.org/10.1002/hyp.10132>
- Zaidi FK, Nazzal Y, Jafri MK, Naeem M, Ahmed I (2015) Reverse ion exchange as a major process controlling the groundwater chemistry in an arid environment: a case study from northwestern Saudi Arabia. *Environ Monit Assess* 187(10):607. <https://doi.org/10.1007/s10661-015-4828-4>
- Zanchi A, Zanchetta S, Berr F, Mattei M, Garzanti E, Molyneux S, Sabouri J (2009) The Eo-Cimmerian (late? Triassic) orogeny in North Iran. *Geol Soc Lond Spec Publ* 312(1):31–55. <https://doi.org/10.1144/SP312.3>
- Zhang Z, Chen X, Huang Y, Zhang Y (2014) Effect of catchment properties on runoff coefficient in a karst area of southwest China. *Hydrological Processes*, 28(11), 3691–3702. <https://doi.org/10.1002/hyp.9920>
- Zhou J, Zhang Y, Zhou A, Liu C, Cai H, Liu Y (2016) Application of hydrochemistry and stable isotopes ($\delta^{34}\text{S}$, $\delta^{18}\text{O}$ and $\delta^{37}\text{Cl}$) to trace natural and anthropogenic influences on the quality of groundwater in the piedmont region, Shijiazhuang, China. *Appl Geochem* 71:63–72. <https://doi.org/10.1016/j.apgeochem.2016.05.018>